# Spatial Characteristics of Continuum X-Ray Emission from Lateral Energy Transport in CO₂-Laser–Produced Plasmas

R. Decoste

*Institut de Recherche d'Hydro-Québec, Varennes, Québec J0L2P0, Canada*

and

J.-C. Kieffer and H. Pépin

*Institut National de la Recherche Scientifique-Energie, Université du Québec, Varennes, Québec J0L2P0, Canada*

A modified layered-target technique is used to provide spatial information about continuum x-ray emission in the plane of an infinite target irradiated by a short-pulse CO₂ laser. Hard x-rays are only observed near or within the laser interaction region. Softer x rays are emitted over a large but shallow area of the target surface. These results are used to discuss lateral energy transport mechanisms.

If laser fusion is to succeed, the laser energy must be transported efficiently from the absorption region to the core of the pellet shell where the rocket effect takes place. Long-wavelength lasers produce abundant suprathermal electrons, which could be used for the inward energy transport. For that purpose, however, one must first find out where the hot-electron energy is transported. Hot-electron trajectories are commonly inferred from either hard continuum x rays[1] or $K\alpha$ emission,[2,3] both due to electron deceleration in the high-density material. Hard x rays with energies near or above the hot-electron temperature are particularly useful in the study of hot-electron lateral energy transport. In this paper, a novel application of layered target techniques[4] is used to provide spatial information on continuum x rays emitted from and below the surface of an *infinite* planar target. In this geometry, which avoids edge effects of finite-size targets,[3,5,6] we find that hard–x-ray emission occurs near or within the laser spot area. By contrast, softer radiation is observed from a large but shallow area of the target surface. The x-ray information is used to discuss possible lateral–energy-transport mechanisms and to obtain some quantitative estimates about hot-electron energy transport.

These experiments were carried out with a CO₂-laser beam (10.6 μm wavelength) incident at 28° on planar half-layered targets described below. The s-polarized laser pulse, 1.5 nsec in duration with a prepulse–to–main-pulse contrast ratio $< 10^{-6}$, was focused on target by an $f/1.5$ off-axis parabolic mirror. The more or less Gaussian-shaped, 90%-energy-spot diameter was measured to be about 200 μm. All the experimental results reported below were obtained at an irradiance of $5 \times 10^{12}$ W/cm², corresponding to the critical flux above which ponderomotive force effects become important.[1,7,8]

First, we describe the experimental procedure to obtain spatial information on lateral x-ray emission from the target surface. Next the technique is extended to provide x-ray information from any plane below the target surface. Basically, spatial information about lateral x-ray emission is obtained through analysis of spatially integrated data. The target is shown schematically in Fig. 1(a). A half-plane layer of a low-$Z$ material [(CH)$_x$ plastic here] is deposited on a higher-$Z$ substrate (glass). In order to minimize possible secondary effects of a step near or within the focal-spot region, the plastic thickness is chosen to be much smaller (~40 times) than the laser-spot diameter, but thick enough to prevent hot electrons from penetrating through the plastic.[1] The time- and space-integrated continuum x-ray emission is recorded with a combination of filter absorber detectors covering the 1–50-keV range.[8] Spatial information is then provided by the relative emission contrast between the weak plastic emitter and the stronger glass emitter area. For example, when the laser is incident on the plastic side near the step, energy transported laterally to the bare glass area next to the plastic step is detected through x-ray emission enhancement by the high-$Z$ material. X-ray emission integrated from different areas of the target surface is obtained by varying the distance $d$ from the laser axis to the plastic step location between shots. Results from three typical x-ray channels are shown in Figs. 1(b)–1(d). When the laser is incident on the plastic side, 600 μm away from the step, an x-ray contribution from the glass
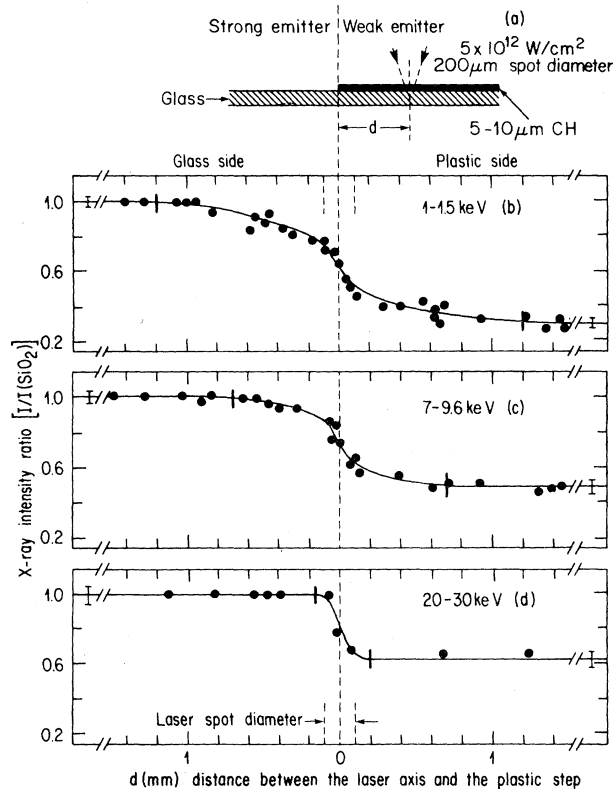
FIG. 1. (a) Schematic of the half-plane layered target used to provide spatial information on lateral x-ray emission. (b), (c), and (d) Space- and time-integrated x-ray emission for three energy channels, obtained by varying the distance between the laser axis and the plastic step location. All signals are normalized to the bare substrate emission corresponding to each channel (statistical error bars on the extreme left). Error bars on the extreme right correspond to the emission from a thick infinite plastic target. The vertical markers are total emission diameters.
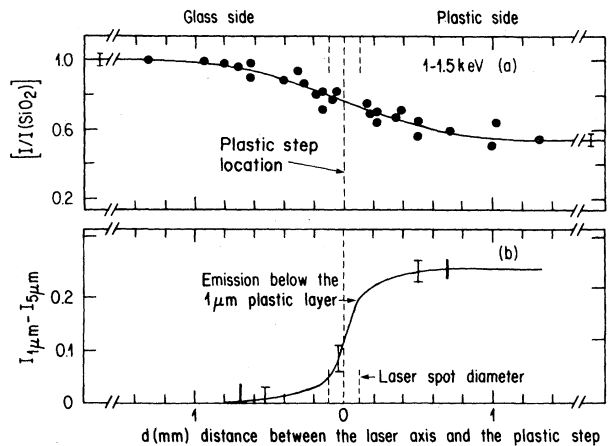


FIG. 2. (a) Space- and time-integrated x-ray emission from a target with a half-plane plastic layer thickness less than the hot-electron penetration depth. The laser axis location is again varied with respect to the plastic step. (b) X-ray emission from the glass substrate below the plastic half plane, obtained by subtracting the 5-$\mu$m [Fig. 1(b)] from the 1-$\mu$m [Fig. 2(a)] distributions. The error bars are due to uncertainties in the data reduction process.

side is already registered on the soft energy channel [Fig. 1(b)] whereas no such contribution is observed on higher-energy channels [Figs. 1(c) and 1(d)]. The more rapid transition in x-ray emission around ± 100 $\mu$m of the step is due to increased x-ray emissivity within the focal-spot area.

With use of the same basic technique, it is also possible to obtain lateral x-ray information from a target plane below a given thickness of plastic. In Fig. 2(a), for example, the thickness of the half-plane plastic layer is reduced to 1 $\mu$m. This is less than the hot-electron penetration into plastic.[1] Therefore, the detectors now register the enhanced x-ray emission from the glass below the plastic, plus the emission from the plastic

layer and the bare glass next to the step. Subtracting the x-ray emission from the target with a thick step [already obtained in Fig. 1(b)] we get, to first order, the x-ray emission from the glass below the 1-$\mu$m plastic layer for different laser axis location with respect to the plastic step [Fig. 2(b)].

The main advantage of the step technique is high sensitivity provided by the spatial integration of the local emissivity over the whole high-$Z$ area of the target surface. Better spatial resolution and even higher sensitivity could be obtained by using a higher-$Z$ substrate such as gold rather than glass.

Interesting information can be obtained through spatial integration of the x-ray emission over different areas of the target surface. A summary of significant results obtained from Figs. 1 and 2 is presented in Table I. At the surface of the target an important fraction of the soft–x-ray emission comes from a region much larger than the laser-spot area, as already observed qualitatively elsewhere.[3,6] Hard x rays, however, are mostly confined to within or near the laser absorption region. As a result, the continuum x-ray emission is softening with increasing distance from the laser interaction region. X rays emitted from the target plane below a 1-$\mu$m layer of plastic show that the soft–x-ray emission ob-

TABLE I. Spatial characteristics of continuum x rays emitted from a planar target. The laser irradiance and spot diameter are $5 \times 10^{12}$ W/cm$^2$ and 200 $\mu$m, respectively.

| X-ray energy (keV) | Emission diameter (mm) | Fractional emission outside the laser spot area |
|---|---|---|
| | Emission from the target surface | |
| 1 - 1.5 | 2.4 | 80% |
| 7 - 9.6 | 1.4 | 60% |
| 20 - 30 | ~0.4 | ~30% |
| | Emission below 1 $\mu$m of plastic | |
| 1 - 1.5 | ~1.4 | ~40% |

served over a large area of the target surface is mostly a shallow surface phenomenon.

Using the x-ray results, we can now try to identify possible lateral–energy-transport mechanisms. Next, quantitative considerations about hot-electron energy transport will be discussed. First, we note that hard x rays imply that the most energetic electrons penetrate the target near or within the laser interaction region. Softer x-ray behaviors could be explained by several energy-transport mechanisms. One possibility is direct energy deposition by less-energetic electrons over a large area of the target surface. These electrons could be flowing to the target along the leading edge of a suprathermal corona in expansion.[5] Direct bombardment of the target surface by hot electrons slowed down by reflections at the potential sheath is also possible. Another approach is a return current, which is necessary to neutralize the outgoing stream of resonantly accelerated electrons.[9] In the process, a closed current loop is established, possibly involving the return of cold or less-energetic electrons[6] from the corona to the target surface outside the laser area. This model has been shown to explain the geometry of magnetic fields observed over a large area of the target surface.[10] Once at the target surface, this return current could also create an x-ray–emitting plasma through Ohmic heating.[11] Interferometry with a short ruby-laser pulse[12] and other observations[5,6] indicate that the diameter of the surface plasma is expanding laterally at a velocity above $10^8$ cm/sec and reaches a diameter comparable to the 1-keV x-ray emission diameter.

Whether long-range lateral energy transport is due to hot electrons with reduced energies or some plasma expansion mechanism is not clear. However, energetic electrons are at least partly

responsible for short-range lateral energy transport, as evidenced by hard x rays. The amount of energy transported by hot electrons can be estimated from x-ray spectra. A typical space- and time-integrated x-ray spectrum obtained under the same conditions as above but with a thick infinite plastic layer is presented in Fig. 3. With use of the results from Table I, this spectrum is reduced to its contribution from within the focal-spot area. Although harder, a two-component spectrum is still observed. Using a simple calculation,[13] we estimate that about 7% of the incident laser energy is transported inward by the hot-electron distribution represented by the hard portion ($>5$ keV) of the spatially integrated spectrum. Approximatively 60% of the inward transport remains within the focal-spot area, and most of the rest can be accounted for within a 200-$\mu$m minor radius beyond the focal spot. Of course, this model does not account for any significant amount of energy possibly dissipated at
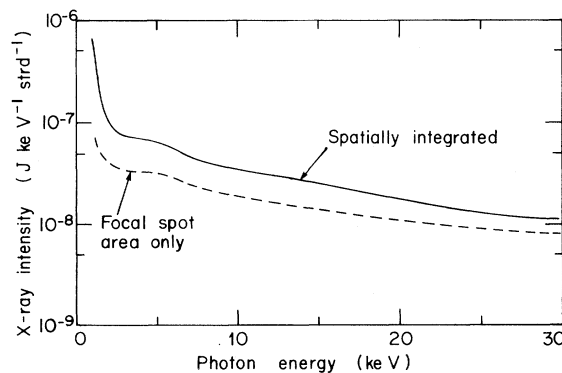


FIG. 3. X-ray emission spectra: Spatially integrated and contribution from the focal-spot area. The integrated spectrum is obtained with six detectors.

the target surface by a return current or any other lateral–plasma-expansion mechanism.[3,5]

In conclusion, spatial information about x-ray emission indicates that the most energetic electrons penetrate the target near or within the laser-interaction region. Most of the energy transported by hot electrons is also limited to a close range around the laser focal spot. Long-range energy transport could be due to hot electrons with reduced energies or some plasma expansion, either suprathermal or Ohmic heating driven, at the target surface. In the context of multibeam irradiation of a pellet surface, our results and others[14] indicate that some laser illumination uniformity is still going to be required when the dominant inward energy-transport mechanism is due to suprathermal electrons. Questions about the overall efficiency of this transport process and whether preheat by the most energetic electrons can be controlled still remain to be addressed.

[1]J. C. Kieffer, H. Pépin, F. Martin, P. Church, T. W. Johnston, and R. Decoste, Phys. Rev. Lett. 44, 1128 (1980).

[2]K. M. Michell and R. P. Godwin, J. Appl. Phys. 49, 3851 (1978); J. D. Hares, J. D. Kilkenny, M. H. Key, and J. G. Lunney, Phys. Rev. Lett. 42, 1216 (1979).

[3]N. A. Ebrahim, C. Joshi, D. M. Villeneuve, N. H. Burnett, and M. C. Richardson, Phys. Rev. Lett. 43, 1995 (1979).

[4]F. C. Young et al., Appl. Phys. Lett. 30, 45 (1977); B. Yaakobi and T. C. Bristow, Phys. Rev. Lett. 38, 350 (1977).

[5]R. S. Marjoribanks, M. D. J. Burgess, G. D. Enright, and M. C. Richardson, Phys. Rev. Lett. 45, 1798 (1980).

[6]P. A. Jaanimagi, N. A. Ebrahim, N. H. Burnett, and C. Joshi, to be published.

[7]D. W. Forslund, J. M. Kindel, and K. Lee, Phys. Rev. Lett. 39, 284 (1977).

[8]H. Pépein et al., J. Appl. Phys. 50, 6784 (1979).

[9]P. Kolodner and E. Yablonovitch, Phys. Rev. Lett. 43, 1402 (1979).

[10]Y. Sakagami, H. Kawakami, S. Nagao, and C. Yamanaka, Phys. Rev. Lett. 42, 839 (1979).

[11]R. F. Benjamin, G. H. McHall, and A. W. Ehler, Phys. Rev. Lett. 42, 890 (1979).

[12]B. Grek, F. Martin, T. W. Johnston, H. Pépin, and G. Mitchell, Phys. Rev. Lett. 41, 1811 (1978); F. Martin, private communication.

[13]The hot-electron distribution is calculated from the hard–x-ray spectrum. As a cross check, the inferred hot-electron distribution is transported through various thicknesses of plastic into a high-$Z$ substrate and the resulting bremmsstrahlung emission is compared with experiments; J. C. Kieffer et al., Bull. Am. Phys. Soc. 25, 1028 (1980).

[14]N. M. Ceglio and J. T. Larsen, Phys. Rev. Lett. 44, 579 (1980).